ELSEVIER

Journal of Alloys and Compounds 253–254 (1997) 195–200

Journal of ALLOYS AND COMPOUNDS

Analysis of FeTi hydride alloys by thermal analysis, small angle neutron scattering and positron annihilation

P.J. Hall[a,*], L.E.A. Berlouis[a], A.J. Mackinnon[a], J. Wilson[b], D. Browning[b], S. Dodd[b], S. Morris[b], P. Jones[b], J.M. Calo[c]

[a]Department of Pure and Applied Chemistry, University of Strathclyde, Glasgow, G1 1XL, Scotland, UK
[b]DRA Hasler, Hasler Road, Gosport, Hampshire, PO12 2AG, England, UK
[c]Division of Engineering, Box D, Brown University, Providence, RI, USA

Abstract

Samples of vapour deposited FeTi and electrochemically loaded with hydrogen from LiOH solution have been examined by thermal analysis, positron annihilation and small angle neutron scattering techniques. Thermal analysis shows that the FeTi loads hydrogen without the need for activation although there was not a good correlation between the amount of hydrogen loaded and duration of loading. Positron annihilation and SANS on the untreated sample showed that the alloy was highly disordered in nature and contained a large concentration of vacancy clusters. SANS also showed an increase in the interfacial scattering surface area following hydrogen loading, consistent with an increase in voidage within the structure. Positron annihilation on the other hand suggested a decrease in the concentration of vacancies following hydrogen loading. It was concluded that some of the voids within the structure were filled by hydrogen gas which caused a decrease in the positron lifetime. However, not all of the voids were filled with gas.

Keywords: FeTi; Small angle neutron scattering; Positron annihilation; Thermal analysis

1. Introduction

From economic arguments, FeTi alloys show considerable potential for commercial development as a hydrogen storage material and there have been a large number of investigations of hydride formation in these systems [1–3]. Even so, there is still a need for detailed information on the kinetics and mechanism of hydrogen absorption to optimize the performance of these materials. One serious limitation in the economics of using of FeTi is the necessity of a prolonged, difficult, and therefore costly, activation process [4]. An activation procedure is required for most metal alloys. In the case of FeTi, the activation process is severe and requires an initial treatment in a reduced pressure of hydrogen at 400 °C followed by hydrogen treatment at 6 MPa and 400 °C. The material may require several cycles of this activation procedure before any uptake of hydrogen is observed. Thereafter hydrogen uptake is undertaken at room temperature under pressure.

As with most alloys, which contain transition metals, the principal mechanism of hydrogen uptake is the formation of a metal hydride. More generally, the formation of a chemical compound is not the only mechanism of gas absorption by metals and the physical trapping of gases is a more common mechanism. Practically all metals contain gas bubbles within their structure and these can have important effects on their mechanical and physical properties [5,6]. The role of gas bubbles in hydrogen storage has not been fully investigated. Gas bubbles are more likely to be formed in disordered materials and in this study the storage properties of an alloy produced by a process which tends to produces disordered products, vapour deposition, are investigated.

Here we present data on the desorption of hydrogen from an electrochemically treated vapour deposited FeTi using differential scanning calorimetry (DSC), thermogravimetric analysis (TGA), and we also examine as received and treated samples using positron annihilation lifetime studies (PAL) and small angle neutron scattering (SANS). While the principles of thermal analysis are widely known, PAL and SANS are less common techniques and a short description will now be given of each.

PAL is a technique that has been widely used to monitor defects in metals, embrittlement of metals by hydrogen and the properties of gas bubbles in metals [7]. The positron is

---

[*] Corresponding author.

0925-8388/97/$17.00
PII S0925-8388(96)02991-X

the anti-particle of the electron and as such has the same mass and spin as the electron but is of the opposite charge. In PALS experiments the positrons are injected into a solid with a mean energy of 200 KeV, and slow down to thermal energies by ionization and excitation of the solid. In most cases the positron will annihilate with emission of γ-quanta and it is the determination of the positron lifetime which forms the basis of this technique [8]. The lifetime of positrons in solid media depends upon the local electronic environment. Generally, the lower the electron density, the longer the lifetime. Lifetimes can be determined by measuring the time difference between the birth of the positron, signalled by the emission of a 1.28 MeV γ-quanta, and the annihilation of the positron, signalled by the emission of a 0.511 MeV γ-quanta. It is the magnitude of this lifetime which is of most interest and can be used to characterise the material under investigation.

SANS is a powerful technique in the investigation of porous materials and can give pore size distributions and the void fraction of solids [9]. Although x-rays are a more readily accessible resource their high absorbance by metals restricts their application to thin films. SANS is the best technique to investigate the large scale properties of metals.

In the realm of published literature there have been few studies that directly compare PAL and SANS techniques. This is somewhat surprising in the sense that these techniques provide an interesting combination of overlapping and complementary information. The most comprehensive investigation was by Eldrup et al. [10] who used PAL and SANS to investigate krypton bubbles in Cu and Ni. In this context, the present work is offered as a study to illustrate the potential of combining these techniques as well as an investigation of the properties of a novel FeTi system.

2. Experimental

Samples of vapour deposited FeTi (prepared by DRA Hasler) were electrochemically treated by having a section of the material as the cathode in an electrochemical cell. The sample was immersed in 0.1M LiOH and two platinum anodes were employed, symmetric with respect to the cathode. A constant current was applied for a specified time and once treatment was complete, the sample was removed, washed with distilled water and dried in a stream of nitrogen. Early evidence of hydriding was given by the brittle and fragile nature of the treated material. The sample was divided to allow DSC, TGA and PAL measurements to be made on the identical loaded material.

Thermal analysis techniques are useful tools in evaluating the kinetic and thermodynamic properties of the desorption process. DSC measurements were made using a Mettler DSC-30 controlled by a Mettler TC-11 interface unit. The DSC instrument uses a highly sensitive sensor with five AuNi thermocouples attached to the sample and reference positions of a glass disc. Approximately 20 mg of sample was loaded into an aluminium pan and 3 pin holes were pierced in the pan lid to allow removal of gaseous products. Heating was conducted from 30 °C to 400 °C at 10 °C min^{-1} under a purge of nitrogen gas with a flowrate of 40 ml min^{-1}. The reference material was a sample of as-received FeTi of similar mass as the treated sample. The sample was scanned twice from 30 °C to 400 °C in succession with the second scan to allow for determination of a baseline.

Thermogravimetric measurements were conducted on a Perkin Elmer TGA 7 thermogravimetric analyzer. Approximately 20 mg of sample was heated from 30 °C to 400 °C at 10 °C min^{-1} under a purge of argon gas at a flowrate of 40 ml min^{-1} and the weight change due to thermal desorption of the hydrogen was automatically recorded on the controlling PC.

Positron annihilation lifetime measurements were carried out using a typical fast–fast spectrometer incorporating plastic scintillators coupled to Hamamatsu photomultiplier tubes (PMT). The positron source was made by drying a droplet of ^{22}NaCl aqueous solution onto a 1 cm^2 section of Kapton (polyimide) foil and securing a similar section of Kapton foil on top to completely seal the source. The source had a strength of approximately 50 μCi. The source was then sandwiched between two sections of the sample which was thick enough to ensure that all positrons annihilated within the metal. Resolution spectra were obtained by using well annealed copper as a reference, which in theory should produce a single well defined lifetime.

A schematic of the PAL spectrometer is illustrated in Fig. 1. Birth and death signals from positrons are detected by the plastic scintillator and photomultiplier combination. The signals from the PMT's are modified by the constant fraction discriminators (CFDD's) to make them suitable as timing signals. Energy selection also takes place by the CFDD's to determine whether the γ-particle is a birth or a death signal. The output from the CFDD's are then used as the start and stop for the time-to-amplitude converter (TAC) whose output is proportional to the time between it receiving a start and stop signal, and hence its output is proportional to the positron lifetime. This signal is digitised by the analogue-to-digital converter (ADC) and fed into one channel of a multi-channel analyzer (MCA). Typically 10^6 annihilations are recorded and the MCA produces a histogram showing the distribution of positron lifetimes, normally referred to as the lifetime spectrum.

Analysis of the spectrum to deconvolute the various lifetime components was carried out using the POSITRONFIT program developed by Eldrup et al. [11]. In this particular instance, the spectra were analyzed in terms of a three component fit.

SANS was performed at the Intense Pulsed Neutron

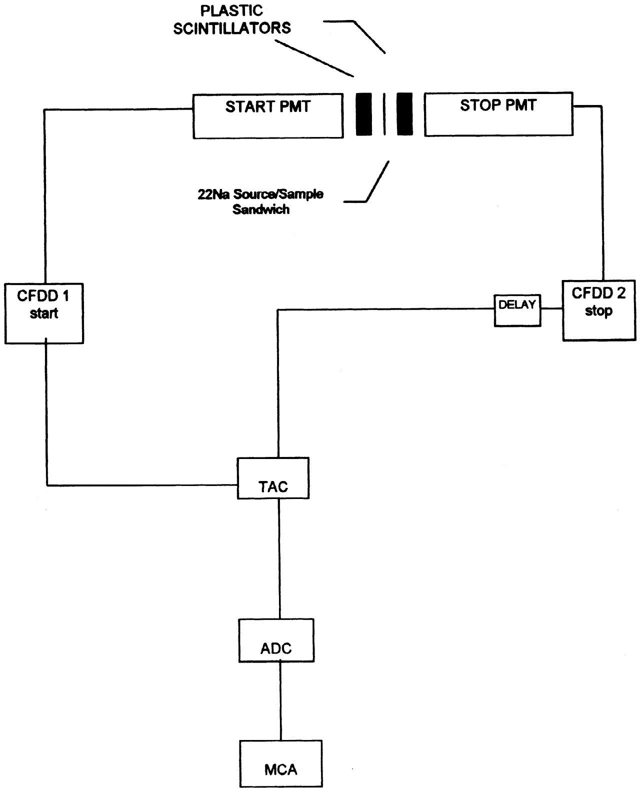

Fig. 1. Schematic of positron annihilation apparatus.

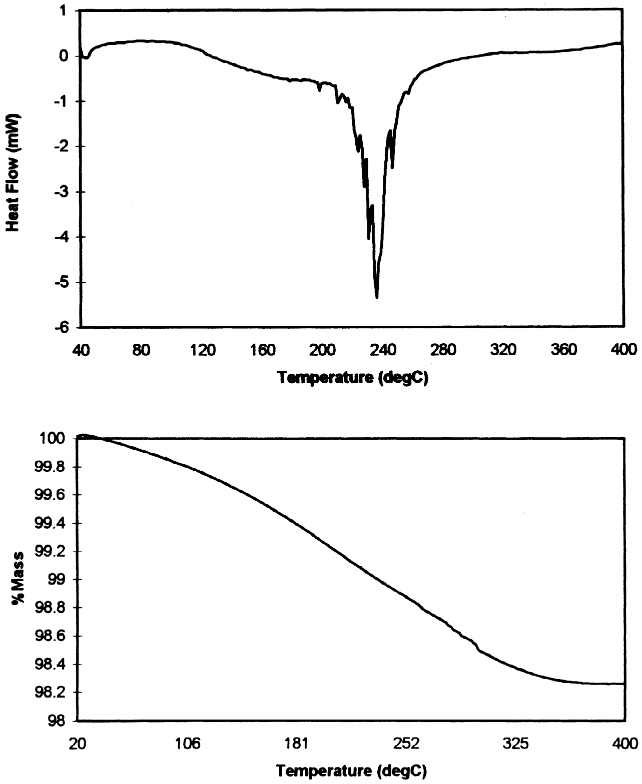

Fig. 2. (a) Differential scanning calorimetry and (b) thermogravimetric analysis at 10 K min^{-1} of FeTi electrochemically loaded with hydrogen at a current density of 100 mA cm^{-2} for 480 h.

Source at the Argonne National Laboratory. In SANS the intensity of scattered neutrons is determined as a function of scattering angle:

$$I = f(q) \tag{1}$$

where q is the scattered wave vector, which is related to the scattered angle, θ, by

$$q = \frac{4\pi}{\lambda}\sin(\theta) \tag{2}$$

The samples were 1 mm thick and the results presented here are corrected for sample thickness and background scattering. When hydrogen was present in the sample, correction for incoherent scattering was made by assuming that at the highest q values available scattering was dominated by incoherent effects and that the magnitude did not vary with scattering angle.

3. Results and discussion

Thermal analysis. Samples of FeTi loaded at various current densities and times were then subjected to the thermal ramp in the DSC and TGA. A typical set of thermograms are displayed in Fig. 1 and the full set of results are summarised in Table 1.

Fig. 2 shows an endothermic event which is consistent with a desorption process. The TGA results in Fig. 2 shows a distinct mass loss. There is no real consistency to the data obtained in Table 1 and much of this may be

Table 1
Summary of DSC and TGA Results

i_d (mA cm^{-2})	t_{load} (hrs)	ΔH(J g^{-1})	T_{peak} (°C)	% mass loss
5.0	23.5	1.4	182.8	0.1
10.0	66.0	86.3	217.6	0.3
10.0	66.5	33.3	217.4	0.7
25.0	67.0	25.2	212.3	1.2
50.0	23.0	26.5	226.9	0.1
100.0	19.5	4.6	197.1	1.0
100.0	25.5	2.4	150.0	0.6
100.0	480.0	25.9	236.2	1.7

Table 2
PAL Results

Sample	τ_1 (ps)	τ_2 (ps)	τ_3 (ps)	σ_1	σ_2	σ_3	I_1 (%)	I_2 (%)	I_3 (%)	σ_1	σ_2	σ_3
Cu	113	180	441	3	–	14	89.4	8.4	2.2	0.8	–	0.1
FeTi	177	445	2611	2	5	88	51.7	46.1	2.2	1.0	0.9	0.8
FeTi–H	189	465	4665	2	5	315	64.0	35.0	1.0	0.8	0.8	0.1

attributed to uncertainties in the determination of the surface area of the sample, necessary for calculating the desired current density and the state of the sample surface. The heat of the desorption process also shows little consistency with the current density and the time of loading. What is clear is that a substantial release of hydrogen is obtained from these electrochemically treated materials and that no activation process is required.

PAL. Table 2 summarises the data obtained for the untreated sample and the sample after electrochemical loading with hydrogen. The PAL spectra have been deconvoluted into three lifetimes. For comparison, the results of a copper standard are also given. The shorter lifetime results from positron annihilation in bulk material and the intermediate one from annihilation in vacancy clusters. These lifetimes are typical for annihilation in metals. The longest lifetime is thought to result from surface trapped positrons but is of low intensity (~1%) and does not convey any useful information about the state of the alloys under investigation. Therefore, positron annihilation in the FeTi is effectively regarded as a two lifetime process.

Following hydrogen loading both of the lifetimes increase but there is a change in relative intensity, with the shorter lifetime becoming more important. The result is that there is a reduction in the mean lifetimes ($\tau = \tau_1 I_1 + \tau_2 I_2$) from 296 ps to 283 ps (±4 ps) following hydrogen loading. In a PAL investigation of hydrogen in iron, Cao et al. [12] worked in terms of mean lifetimes and as such it is difficult to unequivocally interpret their data in terms of the mechanisms of hydrogen absorption. We prefer to work in terms of interpreting changes to the individual lifetimes presented in Table 2. The benefits of our approach should become clear the subsequent discussion.

Small angle neutron scattering. Fig. 3 summarises the SANS measured for the untreated sample, the sample electrochemically loaded with hydrogen and the loaded sample after deloading by heating to 300 °C for 20 min. All three show strong scattering in the small angle region and there are two possible entities for this scattering. The first could be the presence of Fe and Ti crystals in the alloy which have different neutron scattering contrasts. Alternatively, the scattering could be from microvoids formed during the deposition process.

To investigate the crystal structure of the FeTi, wide angle x-ray diffraction (XRD) was performed. This revealed no Bragg peaks, which shows that the FeTi is a highly disordered material containing, at best, crystallites of Fe and Ti less than ~10 Å in size. Therefore, scattering off the neutron contrast between Fe and Ti is not the reason for the intense neutron scattering in the small angle region. Rather scattering is most probably from voids within the structure formed during the vapour deposition process. This is confirmed by the PAL results described above, which show a high proportion of positrons annihilating in voids. In summary, the picture that emerges from XRD, SANS and PAL is that of a highly disordered system with a large void fraction in the structure. The BET surface area of the FeTi determined from N_2 adsorption at 77 K gave a surface area of <1 m^2 g^{-1}. This suggests that most of the surface area of the FeTi is closed to the external surface.

The untreated sample curve linearises on the log–log plot and has a slope of -2.1 indicating scattering from a mass fractal. Mass fractals are defined by the following mass/radius relationship

$$M(r) \alpha r^{D} \qquad (3)$$

where $M(r)$ is the amount of mass within a sphere of radius r for any point within the material and D is the mass fractal dimension. Mass fractals are generally formed from particle aggregates and it appears that the method of formation of the alloys seems to be the formation of small, aggregates which join together to enclosing voids. This is consistent with the alloy having been formed by the vapour deposition technique.

It is not formally possible to compare the void fractions

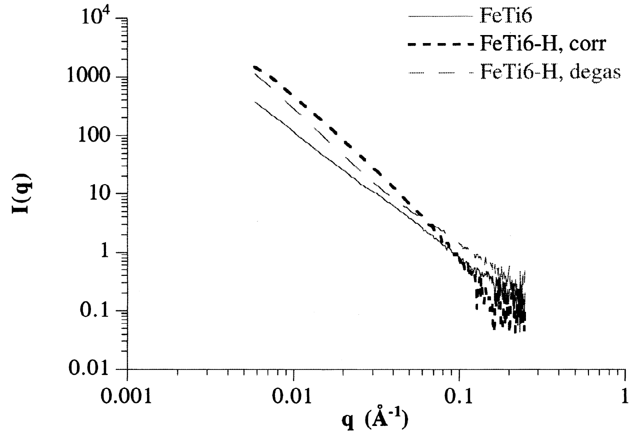

Fig. 3. Small angle neutron scattering for vapour deposited FeTi unloaded, loaded with hydrogen at a current density of 75 mA cm^{-2} for 25 h then deloaded by heating at 300 °C for 20 min.

obtained from Porod scattering invariants ($P = \int I(q)q^2\,dq$) [9] for the untreated and hydrogen loaded FeTi samples because the scattering contrast factor for the hydrogen loaded sample is not known. The reason for this is that (as will be discussed shortly) some of the hydrogen may be present in the form of gas bubbles of unknown pressure. The scattering contrast factor is lower for the hydrogen loaded sample and despite this there is an increase in scattering over most of the q-range. This must be caused by an increase in the interfacial scattering surface area. Notwithstanding this, the Porod invariant for the untreated sample is 0.0020 and for the hydrogen loaded sample the value is 0.0027. This represents a large increase in surface area. A more meaningful comparison is between the untreated sample and the deloaded samples in Fig. 3. The Porod invariant for the deloaded sample is 0.0036 which shows that in the process of hydrogen loading and then deloading there has been an increase in void fraction.

General Discussion. The thermal analysis demonstrates that unlike many FeTi systems, the vapour deposited system investigated here requires little or no activation for hydride formation. This observation is not universally true and for uncertain reasons some samples produced from the same reactor did not respond to electrochemical loading. The reasons for this are unclear but are not likely to be due to the presence of an unreactive oxide layer, because there was no oxygen present during formation.

SANS shows that following hydrogen loading, the interfacial surface area giving rise to scattering increases with a tendency to form larger voids. This is reasonable because the absorbed hydrogen increases the volume of the FeTi sample. Since there is an increase in the surface area in the sample following hydrogen loading, it may be expected that there would be an increase in the lifetime of positrons in voids as well as an increase in the relative intensity of positrons annihilating in voids. Jensen and Nieminen [13] have shown how positron lifetime increases with void size in aluminium and the increase in lifetime for τ_2 in Table 2 following hydrogen loading is explained by this effect. It is also possible to calculate a trapping rate, K for positrons in voids from the PAL data in Table 2 from the following simple relationship [8]

$$K = \frac{I_2(1/\tau_1 - 1/\tau_2)}{(1 - I_2)} \tag{4}$$

K is related to the vacancy concentration, C, by

$$K = \mu C \tag{5}$$

where μ (s^{-1}) is the specific trapping rate and is of the order of 10^{15}. Application of Eq. (2) to the data of Table 2 shows that for the untreated sample $K = 2.91$ ps^{-1} and for the hydrogen loaded sample $K = 1.67$ ps^{-1}. μ varies slowly with void size and it may be assumed that this value does not change from the untreated FeTi to the hydrogen loaded sample. Therefore, the PAL data suggests that there is a reduction of the vacancy sites of the order of 40%. The SANS data however suggests an increase.

The most reasonable explanation for this apparent contradiction is that some of the voids have become filled with hydrogen gas. A number of studies have shown that positron lifetimes in voids within metals are significantly reduced when the void is filled with gas. For example, Jensen and Nieminen [13] have shown a reduction of lifetimes of 400 ps to 190 ps when voids in aluminium were filled with helium Jensen have observed even greater reductions for other gas bubbles [14]. The mechanism for this is an increase in the electron density within the void due to the presence of the gas and in principal it is possible to calculate gas pressures within the voids. A similar effect may be taking place in the FeTi samples following hydrogen loading. The positron lifetime in the FeTi hydride and in the gas filled voids are similar and it is not possible to resolve them within the sensitivity of the PAL technique.

The PAL data for the hydrogen loaded sample therefore suggests that a large fraction of the voids do not contain hydrogen. The reasons for this have yet to be investigated but may be associated with the observation made earlier that certain FeTi samples would lot load electrochemically. It may well be that the surfaces of some of the voids readily dissociate any H_2 present in the void which could then diffuse through the bulk FeTi to other locations.

Following deloading of the hydrogen loaded sample the SANS data in Fig. 3 shows that there is an increase in the void fraction. This could be caused by hydrogen bubbles fracturing the material. It is well known that repeated loading and dissociation of FeTi results in breaking down the structure into a fine powder and SANS is a technique that could monitor this process.

The above discussion shows that hydrogen gas bubbles may play an important role in hydrogen storage in FeTi. As such it may be possible to engineer a material which enhances this effect and thereby increases the performance of the material. If this could be produced then there would be a maximum pressure for storage, which would be dictated by the mechanical properties of the hydride itself.

4. Conclusions

Vapour deposited FeTi is capable of storing hydrogen without the usual activation procedures. PAL and SANS show that the alloy has a highly disordered structure with a high vacancy concentration, there is no significant large scale crystal structure. Following electrochemical loading there is an increase in vacancy concentration and some of the vacancies are filled with hydrogen. Others remain empty for reasons that are not clear. Gas bubbles are therefore important in hydrogen storage in vapour deposited FeTi and it may be possible to engineer materials which enhance this effect.

Acknowledgments

The IPNS is operated under Department of Energy (USA) contract number W-31-109-ENG-38.

References

[1] J.J. Reilly and R.H. Wiswall Jr, *Inorg Chem, 13* (1974) 218.
[2] H. Wenzl and E. Lebsanft. *J. Physics, F10* (1980) 2147.
[3] A.S. Pedersen, P.J. Møller and O.T. Sørensen, *Physica Scripta, T4* (1983) 83.
[4] T. Schober and D.G. Westlake, *Scripta Metallurgica, 15* (1981) 913.
[5] G. Aleford and J. Völkl (eds.), *Hydrogen in Metals* Springer, Berlin, 1978.
[6] S.E. Donnell and J.H. Evans (eds.), *Fundamental Aspects of Inert Gases in Solids* Plenum, New York, 1991.
[7] P. Hautojärvi (ed.), *Positrons in Solids, Topics in Current Physics*, Springer, Berlin, 1979.
[8] M. Eldrup, *J. de Physique IV, 5* (1995) 93.
[9] J.S. Higgins and Benoît, *Polymers and Neutron Scattering*, Oxford Univ. Press, Oxford, 1994.
[10] M. Eldrup, J.S. Pedersen, A. Horsewell, K.O. Jensen and J.H. Evans, in *Fundamental Aspects of Inert Gases in Solids Topics in Current Physics*, Springer, Berlin, 1979.
[11] P. Kirkegaard and M. Eldrup, *Comput. Phys. Comm., 7* (1974) 401.
[12] B. Cao, H. Ichinose, S. Yamamoto, H. Li and Y. Ishida, *Philosophical Magazine A, 67* (1993) 1177.
[13] K.O. Jensen and R.M. Nieminen, *Phys Rev B, 36* (1987) 8219.
[14] K.O. Jensen, M. Eldrup, N.J. Pedersen and J.H. Evans, *J. Phys F, 18* (1988) 1703.